IMAGE INTERPOLATION USING OPTIMIZED COLOR TRANSFORMS

Evgeny Gershikov and Moshe Porat

Department of Electrical Engineering, Technion - Israel Institute of Technology
Technion City, 32000, Haifa, Israel
phone: +972-4-8294725, fax: +972-4-8294799, email: eugeny@tx.technion.ac.il
web: http://vision.technion.ac.il/~eugeny
phone: +972-4-8294684, fax: +972-4-8295757, email: mp@ee.technion.ac.il
web: http://vision.technion.ac.il/mp

ABSTRACT

In many demosaicing algorithms the red and the blue colors are reconstructed based on the interpolated green. Although additional information such as the statistics of the color components could be easily obtained, these algorithms are not optimized according to the available data. In this work we propose optimized color transforms for the reconstruction of the red and blue colors, based on properties of the input image. When comparing the results of the optimized algorithms to existing known techniques, we show improvement in the reconstructed images both visually and according to the S-CIELAB quality measure. Based on extensive simulation results, we show and conclude that the proposed optimization techniques could be useful and instrumental in digital photography.

1. INTRODUCTION

Image interpolation has been researched intensively recently. In particular, the problem of demosaicing has attracted attention due to its role in many acquisition devices. In demosaicing a full color image is reconstructed from a single image, where at each pixel only one of the primary colors: R (red), G (green) or B (blue) is known. Usually a Bayer Color Filter Array (CFA) pattern [1] is used as shown in Fig. 1. In order to obtain the image in full color, the missing color values (50% of the green and 75% of the red and blue pixels) have to be reconstructed using the available information. Naturally, the high correlations of the RGB colors in most images [2], [3] should be considered in the reconstruction process.
This problem can be solved by the straightforward methods of nearest neighbor (pixel replication), bi-linear (neighbor averaging), bi-cubic or bi-spline interpolation methods, where each component is processed independently. However, higher image quality is expected if also the inter-color correlations are exploited. One way to do so is to reconstruct the red and blue colors using the green (which is reconstructed first) as done in sequential demosaicing methods [4]. This is motivated by the fact that G has twice more samples than R or B in the Bayer CFA pattern. Such algorithms are presented, for example, in [5], [6], [7], [8], [9] and [10]. Much effort has been invested in such algorithms to the reconstruction of the green, both because it is closest to the luminance information of the image and since errors in its reconstruction are propagated to the chrominance channels (R and B). However, the quality of interpolation of the chrominance information of the image is also important for high performance of the overall demosaicing algorithm, as shown in this work.

Other non-sequential algorithms may apply an iterative approach to demosaicing of refining G and R/B together, e.g., using color ratios [11] or color differences [12] or employ simultaneous modelling of the three colors [13].
We start with analyzing a basic demosaicing method. Statistical and other methods for its optimization are introduced in Sections 2 and 3, respectively.

1.1 The basic demosaicing method

In the basic demosaicing method we use the technique proposed in [10] for R and B interpolation. For the presentation of this technique, the input Charged Coupled Device (CCD) image is considered as made of four input images according to color: *RR* for the red, *BB* for the blue and *GR* and *GB* for the green (see Fig. 1). Also for each pixel two types of neighbors are considered, namely 'x' type neighbors and '+' type neighbors (Fig. 2). The idea in [10] is to learn the relationships between a pixel p and its ('x' or '+' type) neighbors n_i in the small images (e.g., *GR*, *GB*) and then use these relationships to reconstruct the missing pixels. A linear approximation is used, i.e.

$$p = \sum_i \alpha_i n_i, \tag{1}$$

where i runs on the neighbors and α_i is the coefficient corresponding to n_i in the expansion. The learned expansion coefficients α_i are used to build the interpolated image in separate stages for pixels with known 'x' type neighbors and pixels with known '+' type neighbors. The expansion coefficients are chosen to be optimal in the Least Squares (LS) sense. For a group of pixels a linear system of equations is built: $\mathbf{p} = \mathbf{N}\alpha$, where $\mathbf{p}$ is the pixel vector, α is the coefficient vector and $\mathbf{N}$ is the neighbor matrix. The solution of this system in the LS sense is $\alpha = \left(\mathbf{N}^T\mathbf{N}\right)^{-1}\mathbf{N}^T\mathbf{p}$. The groups
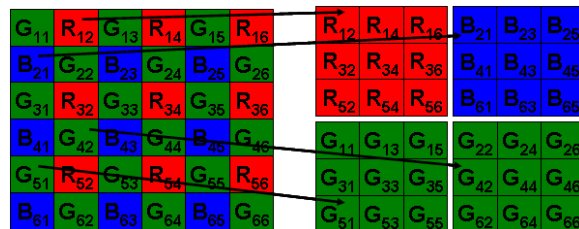

Figure 1: **The Bayer CFA pattern (left) and the input images (right): RR, BB (top row from left to right), GR, GB (bottom row).**

x	+	x
+	p	+
x	+	x

Figure 2: 'x' type and '+' type neighbors of a pixel p.

of pixels on which the LS optimization is performed correspond to the image regions. These regions are the result of image segmentation based on the relationships between the intensity values of the neighbors of a given pixel. Thus the pixels of each region are not necessarily spatially adjacent. The stages of the basic demosaicing method follow.

1. The green color component is interpolated using the edge sensitive method introduced in [5]. The technique includes filtering the CFA pattern horizontally and vertically and choosing either the horizontal interpolator, the vertical one or the average of the two according to the direction of the smaller one of the estimated horizontal and vertical gradients. Other more sophisticated methods of combining the horizontal and vertical interpolators have been recently proposed [7], [8], however for simplicity we use the original technique.

2. The red and the blue colors are reconstructed using the interpolated green component $\hat{G}_1$. The color differences $\Delta_1^{RG} \triangleq R_{CCD} - \hat{G}_1$, $\Delta_1^{BG} \triangleq B_{CCD} - \hat{G}_1$ are considered, where R_{CCD} and B_{CCD} are the original CCD pixels of the red and the blue colors, respectively. The differences are reconstructed at the locations of pixels, where the 'x' type neighbors are known, using the relationships with these neighbors. The reconstructed color differences are denoted Δ_2^{RG} and Δ_2^{BG}.

3. Again the pixels at the same locations as in Step 2 are reconstructed to achieve higher accuracy of the algorithm. The color difference $\Delta_1^{RB} \triangleq \Delta_2^{RG} - \Delta_2^{BG}$ is calculated and reconstructed at odd row, even column positions using the relationships learned from the even row, odd column positions (with their 'x' type neighbors) and vice versa. The result is Δ_2^{RB}, used to derive the R and B values ($\hat{R}_1$ and $\hat{B}_1$).

4. The remaining missing pixels of the red and the blue are reconstructed using again the color differences $\Delta_3^{RG} = \hat{R}_1 - \hat{G}_1$ and $\Delta_3^{BG} = \hat{B}_1 - \hat{G}_1$ and the relationships with their '+' type neighbors. The results are Δ_4^{RG} and Δ_4^{BG}.

5. The final red and blue components are calculated according to $\hat{R}_2 = \hat{G}_1 + \Delta_4^{RG}$, $\hat{B}_2 = \hat{G}_1 + \Delta_4^{BG}$. The output of the algorithm is $(\hat{R}_2, \hat{G}_1, \hat{B}_2)$.

2. STATISTICAL OPTIMIZATION METHODS

As can be seen above, the basic method uses the differences R-G, B-G in Steps 2 and 4. This choice is rather arbitrary and other combinations of the colors can be considered, so that the color components are, for example, more de-correlated. The color transform can be, actually, chosen to optimally achieve some desired property [14], [15]. Since more than half of the pixel values are missing in the input image it is difficult to apply a color transform at the very beginning of the algorithm. However, after the reconstruction of the green it is possible. Thus, in Steps 2 and 4 we propose the following generalization:

$$C_1 = G, \quad C_2 = a_1 R + a_2 G, \quad C_3 = d_1 B + d_2 G \quad (2)$$

for some constants a_1, a_2, d_1, d_2. Note that we do not include B in C_2 or R in C_3 because R and B are known at totally different pixel locations in the CCD image. We consider several choices of the a and d coefficients.

2.1 Minimal variances of C_2 and C_3

The idea is to look for a_1 and a_2 that minimize the variance of C_2 and for d_1 and d_2 that minimize the variance of C_3. Clearly, if the variance of C_2 becomes zero the algorithm will introduce no error in the interpolation of the red color. Similarly for C_3 and the blue. In order to avoid the trivial choice of $a_1 = a_2 = 0$ or $d_1 = d_2 = 0$, a constraint has to be added that can force, for example, the L1 or L2 norm of the a and d coefficients to be 1, i.e.,

$$\begin{aligned} |a_1| + |a_2| = 1, \quad &|d_1| + |d_2| = 1 \quad \text{or} \\ a_1^2 + a_2^2 = 1, \quad &d_1^2 + d_2^2 = 1. \end{aligned} \quad (3)$$

The expressions for the variances are

$$\begin{aligned} var(C_2) &= a_1^2 var(R) + 2a_1 a_2 cov(R,G) + a_2^2 var(G) \\ var(C_3) &= d_1^2 var(B) + 2d_1 d_2 cov(B,G) + d_2^2 var(G) \end{aligned} \quad (4)$$

and these are minimized under one of the constraints of (3). $var()$ stands here for variance and $cov()$ for covariance. The solution under the L1 norm constraint for a_1 and a_2 is

$$\begin{aligned} a_1 &= \frac{cov(R,G) + var(G)}{var(R) + 2cov(R,G) + var(G)} \\ a_2 &= -\frac{cov(R,G) + var(R)}{var(R) + 2cov(R,G) + var(G)}. \end{aligned} \quad (5)$$

The solution for d_1 and d_2 is the same as (5) except that R should be replaced everywhere by B.

2.2 Minimal covariance of C_2 and C_3

Here we search for the values of a_1, a_2 and d_1, d_2 that minimize the covariance of C_2 and C_3, given by

$$\begin{aligned} cov(C_2, C_3) =& a_1 d_1 cov(R,B) + a_1 d_2 cov(R,G) \\ &+ a_2 d_1 cov(B,G) + a_2 d_2 var(G). \end{aligned} \quad (6)$$

The same constraints of (3) can be used. Under the L1 norm constraint the a_1, a_2 solution follows (similarly for d_1, d_2).

$$\begin{aligned} a_1 &= \frac{cov(B,G) + var(G)}{cov(R,G) + cov(B,G) + cov(R,B) + var(G)} \\ a_2 &= -\frac{cov(R,G) + cov(R,B)}{cov(R,G) + cov(B,G) + cov(R,B) + var(G)}. \end{aligned} \quad (7)$$

The motivation for this optimization is similar to the one for using de-correlating color transforms in image compression: concentration of most of the energy of C_2 and C_3 in one of them to reduce the reconstruction errors.

2.3 Gram-Schmidt orthogonalization

The idea of de-correlation of Subsection 2.2 can be viewed as orthogonalization using the inner product of $\langle C_1, C_2 \rangle = cov(C_1, C_2)$. We can use the Gram-Schmidt process for such orthogonalization. The problem is that if we start with C_2 and C_3 as in (2) for some non-zero values of a_1 and d_1, we will get as a result linear combinations where both R and B are present. An alternative is to consider the orthogonalization of R, G and B, G separately. We start with G and project R on it and similarly, for B and G orthogonalization, B is projected on G. Now we propose to take these two vectors as C_2 and C_3, i.e., under the L1 norm constraint in (3)

$$a_1 = \frac{var(G)}{var(G) + cov(R, G)}, \ a_2 = -\frac{cov(R, G)}{var(G) + cov(R, G)},$$
$$d_1 = \frac{var(G)}{var(G) + cov(B, G)}, \ d_2 = -\frac{cov(B, G)}{var(G) + cov(B, G)}. \tag{8}$$

Note that although $cov(C_1, C_2) = cov(C_1, C_3) = 0$ we do not expect that $cov(C_2, C_3) = 0$ using this choice of the coefficients, but C_2 and C_3 usually become de-correlated since it can be shown that

$$cov(C_2, C_3) = cov(a_1 R + a_2 G, d_1 B + d_2 G)$$
$$= var(G)\frac{var(G)cov(R, B) - cov(R, G)cov(B, G)}{(var(G) + cov(R, G))(var(G) + cov(B, G))} \tag{9}$$
$$= \frac{\sqrt{var(R)var(B)}}{\left(1 + \frac{cov(R, G)}{var(G)}\right)\left(1 + \frac{cov(B, G)}{var(G)}\right)}(\rho_{RB} - \rho_{RG}\rho_{BG}),$$

which can be expected to be small. ρ_{RB} denotes here the correlation of R and B and similarly for ρ_{RG} and ρ_{BG}.

It is of interest that the Gram Schmidt process described here is the solution of two other problems as presented next.

2.3.1 Minimizing the covariance of $R - \alpha G$ and $B - \beta G$

Considering the simplified choice of $C2 = R - \alpha G$ and $C3 = B - \beta G$ and taking the covariance of the two we get that

$$cov(C_2, C_3) = cov(R, B) - \beta cov(R, G)$$
$$- \alpha cov(B, G) + \alpha \beta var(G). \tag{10}$$

Minimizing (10) for α and β results in the solution

$$\alpha = \frac{cov(R, G)}{var(G)}, \quad \beta = \frac{cov(B, G)}{var(G)}, \tag{11}$$

which is the same as in (8) up to a scale parameter.

2.3.2 Minimizing the correlation of $R - \alpha G$ and $B - \beta G$

We consider the correlation of $C2 = R - \alpha G$ and $C3 = B - \beta G$ given by

$$corr(C_2, C_3) = \frac{cov(C_2, C_3)}{\sqrt{var(C_2)var(C_3)}}. \tag{12}$$

The expression for $cov(C_2, C_3)$ is given in (10) and the variances are given by

$$var(C_2) = var(R) - 2\alpha cov(R, G) + \alpha^2 var(G)$$
$$var(C_3) = var(B) - 2\beta cov(B, G) + \beta^2 var(G). \tag{13}$$

It can be shown that the solution of this problem is once again as in (11).

3. OPTIMAL SMOOTHNESS OF C_2 AND C_3

The reason that many algorithms use the $R - G$ and $B - G$ differences to reconstruct R and B is that these differences are primarily low pass signals [7]. This means that $R - G$ and $B - G$ are smooth or have low gradients in the spatial domain. Furthermore, this fact can be exploited in the estimation process of the missing pixels by using, for example, bilinear interpolation of the differences [7], [8], [9]. To further impose this smoothness on C_2 and C_3, the following methods are proposed.

3.1 Minimal high pass energy

The idea here is to minimize the energy of C_2 and C_3, filtered by a two dimensional High Pass (HP) filter. We denote the filtered color components by C_k^{HP} and minimize $\sum_{i=1}^{M}\sum_{j=1}^{N}\left(C_k^{HP}\right)_{ij}^2$, $k = 2, 3$ for an image of size $M \times N$. Alternatively, a pair of one dimensional HP filters HP_x and HP_y can be used to filter C_2/C_3 horizontally and vertically, respectively. Usually, HP_y is chosen as $HP_y = HP_x^T$. Then the expression to be minimized becomes $\sum_i \sum_j \left(C_k^{HP_x}\right)_{ij}^2 + \sum_i \sum_j \left(C_k^{HP_y}\right)_{ij}^2$, $k = 2, 3$, where $C_k^{HP_x}$ is C_k filtered by HP_x and similarly for $C_k^{HP_y}$. The optimal a_1, a_2 coefficients for this problem under the L1 norm constraint in (3) are

$$a_1 = \frac{\alpha_{12} + \alpha_{22}}{\alpha_{11} + 2\alpha_{12} + \alpha_{22}}, \quad a_2 = -\frac{\alpha_{12} + \alpha_{11}}{\alpha_{11} + 2\alpha_{12} + \alpha_{22}}, \tag{14}$$

where

$$\alpha_{11} \triangleq \sum_i \sum_j \left[\left(R^{HP_x}\right)_{ij}^2 + \left(R^{HP_y}\right)_{ij}^2\right],$$
$$\alpha_{22} \triangleq \sum_i \sum_j \left[\left(G^{HP_x}\right)_{ij}^2 + \left(G^{HP_y}\right)_{ij}^2\right] \quad \text{and} \tag{15}$$
$$\alpha_{12} \triangleq \sum_i \sum_j \left[\left(R^{HP_x}\right)_{ij}\left(G^{HP_x}\right)_{ij} + \left(R^{HP_y}\right)_{ij}\left(G^{HP_y}\right)_{ij}\right].$$

The solution for the d_1 and d_2 coefficients is the same as the solution for a_1 and a_2, respectively, (in (14)) with B replacing R everywhere in (15). For simple choices of HP_x, such as the backward/forward approximation of the horizontal derivative ($HP_x = [1 - 1]$), the calculations can be performed on the available small images obtained from the CFA (Fig. 1). Alternatively, R and B can be first reconstructed using some simple technique, such as bilinear filtering of the $R - G$ and $B - G$ differences and then used for the estimation of the derivatives. In this work we use the Sobel gradient operator given by $HP_x = \begin{pmatrix} 1 & 0 & -1 \\ 2 & 0 & -2 \\ 1 & 0 & -1 \end{pmatrix}$.

3.2 Minimal energy in the frequency domain

Another approach is to consider the energy of C_2 and C_3 color components in the frequency domain. To impose optimal smoothness we look for the coefficients a_1, a_2, d_1 and d_2 that minimize the energy in the high frequencies. One possible formulation for this problem is to minimize $\int_{\pi/2}^{\pi} \int_{\pi/2}^{\pi} |F^{C_k}(\theta_1, \theta_2)|^2 d\theta_1 d\theta_2$, $k = 2, 3$, where F^{C_k} is the

Fourier transform of C_k. The solution for this problem is the same as in (14), where the α_{11}, α_{12} and α_{22} parameters are

$$\alpha_{11} \triangleq \int_{\pi/2}^{\pi} \int_{\pi/2}^{\pi} |F^R(\theta_1, \theta_2)|^2 d\theta_1 d\theta_2,$$

$$\alpha_{22} \triangleq \int_{\pi/2}^{\pi} \int_{\pi/2}^{\pi} |F^G(\theta_1, \theta_2)|^2 d\theta_1 d\theta_2 \quad \text{and} \qquad (16)$$

$$\alpha_{12} \triangleq \int_{\pi/2}^{\pi} Re\left(F^R(\theta_1, \theta_2)\left(F^G(\theta_1, \theta_2)\right)^*\right) d\theta_1 d\theta_2.$$

Here $Re()$ denotes the real part of a complex number and $*$ is the complex conjugate operator. Also in our implementation the Discrete Fourier Transform (DFT) is used, so that the integrals $\int_{\pi/2}^{\pi} \int_{\pi/2}^{\pi} (\cdot) d\theta_1 d\theta_2$ are replaced by $\sum_{M/4}^{M/2-1} \sum_{N/4}^{N/2-1}$ on the DFTs of the signals (assuming their size is $M \times N$). To calculate the DFTs, R and B are first reconstructed as proposed in Subsection 3.1. Usually, the small matrices RR and BB cannot be used for the DFTs because of aliasing produced by the CFA sampling in the red and the blue colors.

4. SIMULATIONS

First we discuss the comparison of the techniques based on the optimization proposed in Sections 2 and 3. The demosaicing results for a set of images are shown in Table 1. The distortion measure used is the spatially extended CIELAB (S-CIELAB [16]) with 25 samples/degree. The demosaicing results of all the algorithms were refined by the technique proposed in [17]. As can be seen from Table 1, all the proposed methods improve the performance of the basic method. The best one among them is the algorithm that minimizes HP energy (Min HP). Also among the statistical methods the Gram-Schmidt algorithm is better than the algorithms minimizing the covariance or the variances of C_2 and C_3. This means de-correlation by itself is not a sufficient optimization criterion [14]. Similarly, just minimizing the variances is not optimal. The non-singularity of the color transform is also important as ensured by the Gram Schmidt method.

For comparison of this algorithm to other available techniques we have taken several of the algorithms that achieve the best performance according to [4]: Projection on Convex Sets (POCS [6]), Adaptive Filtering (AF [18]), Directional Linear minimum mean square error (DL [7]), Local Polynomial Approximation (LPA [9]), Variance of Color Differences (VCD [8]) and Color Correlation Approach (CCA [19]) with post-processing [20]. Their performance is shown in the right part of Table 1. As can be seen, the Min HP algorithm is superior to the other methods. This can be further seen in Fig. 3 where demosaicing results for part of the fourth image in Table 1 are shown. Note the artifacts on the red coat, least noticeable for the proposed methods.

5. SUMMARY AND CONCLUSIONS

We have proposed new optimized color transforms for image demosaicing. These transforms are used to convert the RGB color components to an alternative color space, where the reconstruction of the missing pixels is performed. The optimization is based on major statistical properties of the new color components, such as minimal variances or minimal covariance. This increases the energy compactness of the color components and reduces the demosaicing error. The smoothness of the color components can be increased as well, mea-
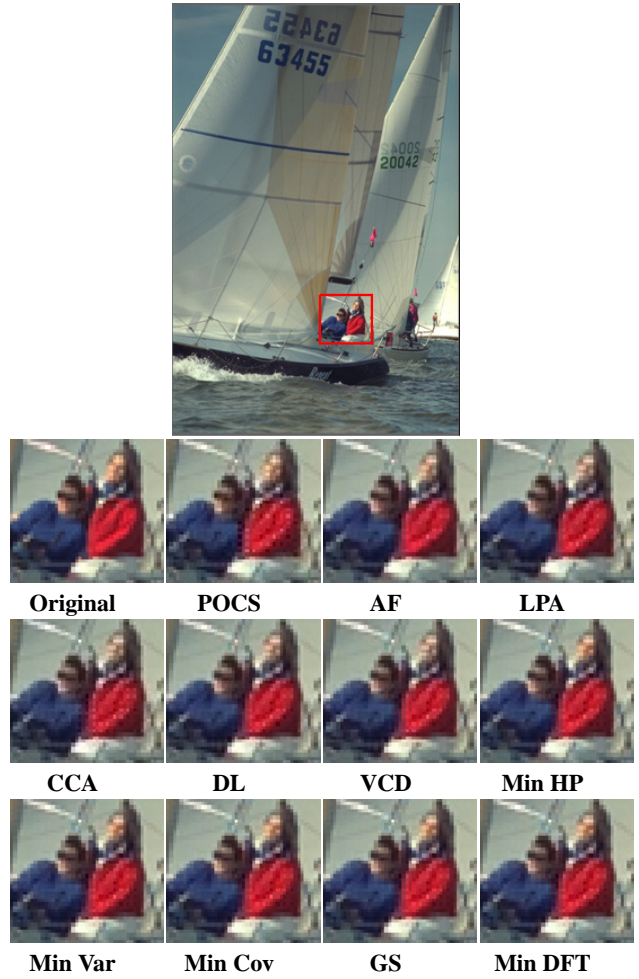

Figure 3: **Demosaicing results for the different algorithms for the fourth image in Table 1. Min HP and the bottom row are the new algorithms. GS stands for Gram-Schmidt.**

sured in terms of the energy in the high frequencies, either in the image or the Fourier transform domain. Since many demosaicing techniques rely on the smoothness of the interpolated colors, this also improves the interpolation performance.

We present simulations results of a basic interpolation method, with and without optimization of its color transform. Having compared the performance of our algorithms to other available demosaicing techniques, it can be shown that the algorithm that minimizes the energy in the high frequencies in the image domain is superior to all the other methods both with respect to the S-CIELAB metric and to visual evaluation. Our conclusion is that optimization of color transforms could be instrumental and helpful in image demosaicing tasks.

Image	New Algorithms						Existing Algorithms					
	Min HP	Min Var	Min Cov	Gram Schmidt	Min DFT	Basic	POCS	AF	DL	LPA	VCD	CCA
	0.5485	0.5579	0.5713	0.5652	0.5814	0.5865	0.8826	0.5880	0.5812	0.5615	0.5880	0.8418
	0.7557	0.7546	0.7600	0.7605	0.7723	0.7749	1.0419	0.7716	0.7598	0.7647	0.7458	0.9640
	1.6152	1.6301	1.6363	1.6300	1.7326	1.7338	2.0024	1.6244	1.7942	2.2520	1.6870	2.1220
	0.5329	0.5356	0.5263	0.5261	0.5716	0.5754	0.8147	0.5675	0.5774	0.5788	0.5563	0.8097
	0.8663	0.8666	0.8839	0.8782	0.8901	0.8951	1.1585	0.8585	0.8738	0.8705	0.9335	1.0872
	1.4234	1.4439	1.5073	1.4808	1.4261	1.4228	1.7269	1.4376	1.4970	1.5408	1.6777	1.8649
	1.2609	1.3149	1.2473	1.2464	1.3230	1.3349	1.4314	1.2993	1.2925	1.6054	1.2073	1.5139
	0.9743	1.0687	0.9904	1.0001	1.0236	1.0180	1.1793	0.9903	0.9760	1.0060	0.9741	1.1040
Mean	**0.9972**	**1.0215**	**1.0153**	**1.0109**	**1.0401**	**1.0427**	**1.2797**	**1.0171**	**1.0440**	**1.1475**	**1.0462**	**1.2884**

Table 1: **S-CIELAB results for the algorithms (from left to right): minimal HP energy, minimal variance, minimal covariance, Gram-Schmidt, minimal DFT energy, the basic method, POCS [6], AF [18], DL [7], LPA [9], VCD [8] and CCA [19].**

REFERENCES

[1] B. E. Bayer, "Color imaging array", U.S. Patent 3971065, July 1976.

[2] H. Yamaguchi, "Efficient Encoding of Colored Pictures in R, G, B Components", *IEEE Trans. on Communications*, vol. 32, pp. 1201–1209, Nov. 1984.

[3] Y. Roterman and M. Porat, "Color Image Coding using Regional Correlation of Primary Colors", *Elsevier Image and Vision Computing*, vol. 25, pp. 637–651, 2007.

[4] X. Li, B. Gunturk and L. Zhang, "Image Demosaicing: A Systematic Survey", *Proc. of SPIE*, vol. 6822, pp. 68221J–68221J-15, 2008.

[5] J. F. Hamilton and J. E. Adams, "Adaptive Color Plane Interpolation in Single Sensor Color Electronic Camera", U.S. Patent 5629734, 1997.

[6] B. K. Gunturk, Y. Altunbasak and R. M. Mersereau, "Color plane interpolation using alternating projections", *IEEE Trans. Image Proc.*, vol. 11, pp. 997–1013, 2002.

[7] L. Zhang and X. Wu, "Color Demosaicking via Directional Linear Minimum Mean Square-Error Estimation", *IEEE Trans. on Image Processing*, vol. 14, no. 12, pp. 2167–2178, 2005.

[8] K.-H. Chung and Y.-H. Chan, "Color Demosaicing Using Variance of Color Differences", *IEEE Trans. on Image Processing*, vol. 15, no. 10, pp. 2944–2955, 2006.

[9] D. Paliy, V. Katkovnik, R. Bilcu, S. Alenius, and K. Egiazarian, "Spatially Adaptive Color Filter Array Interpolation for Noiseless and Noisy Data", *Int. Journal of IS&T*, vol. 17, no. 3, pp. 105-122, 2007.

[10] R. Sher and M. Porat, "CCD Image Demosaicing using Localized Correlations", in *Proc. of EUSIPCO*, 2007.

[11] R. Kimmel, "Demosaicing: Image Reconstruction from Color CCD Samples," IEEE Trans. Image Proc., vol. 8, no. 9, pp. 1221–1228, 1999.

[12] C.-Y. Su, "Highly effective iterative demosaicing using weighted-edge color-difference interpolations", *IEEE Trans. Consum. Electron.*, vol. 52, pp. 639–645, 2006.

[13] C. Kwan and X. Wu, "A classification approach to color demosaicing", *Proc. ICIP*, pp. 2415–2418, 2004.

[14] E. Gershikov and M. Porat, "On Color Transforms and Bit Allocation for Optimal Subband Image Compression", *Signal Processing: Image Communication*, vol. 22, no. 1, pp 1–18, Jan. 2007.

[15] E. Gershikov, E. Lavi-Burlak and M. Porat, "Correlation-Based Approach to Color Image Compression", *Signal Processing: Image Communication*, vol. 22, no. 9, pp. 719–733, Oct. 2007.

[16] X. Zhang and B. A. Wandell, "A spatial extension of cielab for digital color image reproduction", *SID Journal*, 1997. [Available: http://white.stanford.edu/~brian/scielab/scielab.html].

[17] L. Chang and Y.-P. Tan, "Effective use of spatial and spectral correlations for color filter array demosaicing", *Trans. Consum. Electron.*, vol. 50, pp. 355-365, 2004.

[18] N.-X. Lian, L. Chang, Y.-P. Tan and V. Zagorodnov, "Adaptive filtering for color filter array demosaicking", *Trans. Image Proc.*, vol. 16, pp. 2515–2525, 2007.

[19] R. Lukac, K.N. Plataniotis, D. Hatzinakos, and M. Aleksix, "A novel cost effective demosaicing approach", *IEEE Trans. Consum. Electron.*, vol. 50, no. 1, pp. 256–261, 2004.

[20] R. Lukac, K. Martin and K.N. Plataniotis, "Demosaicked image postprocessing using local color ratios", *Trans. Cir. Sys. Video Tech.*, vol. 14, pp. 914–920, 2004.